Practice article

Health-aware control design based on remaining useful life estimation for autonomous racing vehicle

Fatemeh Karimi Pour [a,*], Didier Theilliol [b], Vicenç Puig [a], Gabriela Cembrano [a]

[a] *Advanced Control Systems Group, Universitat Politècnica de Catalunya, Institut de Robòtica i Informàtica Industrial (CSIC-UPC), C/. Llorens i Artigas 4-6, 08028 Barcelona, Spain*
[b] *Universite de Lorraine, CRAN CNRS, UMR 7039, Campus Sciences, B.P. 70239, 54506 Vandoeuvre-les-Nancy Cedex, France*

ABSTRACT

The accurate estimation of the State of Charge (SOC) and an acceptable prediction of the Remaining Useful Life (RUL) of batteries in autonomous vehicles are essential for safe and lifetime optimized operation. The estimation of the expected RUL is quite helpful to reduce maintenance cost, safety hazards, and operational downtime. This paper proposes an innovative health-aware control approach for autonomous racing vehicles to simultaneously control it to the driving limits and to follow the desired path based on maximization of the battery RUL. To deal with the non-linear behavior of the vehicle, a Linear Parameter Varying (LPV) model is developed. Based on this model, a robust controller is designed and synthesized by means of the Linear Matrix Inequality (LMI) approach, where the general objective is to maximize progress on the track subject to win racing and saving energy. The main contribution of the paper consists in preserving the lifetime of battery and optimizing a lap time to achieve the best path of a racing vehicle. The control design is divided into two layers with different time scale, path planner and controller. The first optimization problem is related to the path planner where the objective is to optimize the lap time and to maximize the battery RUL to obtain the best trajectory under the constraints of the circuit. The proposed approach is formulated as an optimal on-line robust LMI based Model Predictive Control (MPC) that steered from Lyapunov stability. The second part is focused on a controller gain synthesis solved by LPV based on Linear Quadratic Regulator (LPV-LQR) problem in LMI formulation with integral action for tracking the trajectory. The proposed approach is evaluated in simulation and results show the effectiveness of the proposed planner for optimizing the lap time and especially for maximizing the battery RUL.

1. Introduction

In the last decades, autonomous driving technology has become a research field of interest for the automotive industry. Autonomous driving technology is anticipated to decrease driver errors, prevent possibly dangerous situations and simplify the driver's work [1,2]. The advanced driver assistance systems (ADAS) or even autonomous driving are a fast developing fields, with increasing interest in both industry and academia. ADAS can be found nowadays in many commercial vehicles such as cruise control or lane keeping which are based on classic control strategies [3]. However, lateral control of an autonomous vehicle still needs to be more investigated because of the difficulties it poses.

The recent research on autonomous driving incorporates different fields, including perception, planning, and control. The purpose of perception is to acquire information for autonomous vehicles regarding its localization in the environment. The goal of control is to obtain the suitable parameters for systems to follow the planned path and planning is the decision-making frame between perception and control [4,5]. The specific object of planning is to the steer vehicle with a safe and without collision path to their destination, considering vehicle dynamics and road lines. Path planning has been widely investigated in mobile robotics applications [6]. In [7], the grid-based approach is used for dynamic path planning where the environment is planned to a set of cells and each cell describes the behavior of an obstacle at that situation in the environment. A hierarchical path planning approach for mobile robot navigation in complex situations is presented in [8]. Both approaches perform well for path planning in low-speed applications but are not suitable for high-speed driving. The artificial potential fields method where stream functions are applied to plan the paths of autonomous vehicles is provided in [9].

* Corresponding author.
E-mail addresses: fkarimi@iri.upc.edu (F. Karimi Pour), didier.theilliol@univ-lorraine.fr (D. Theilliol), vpuig@iri.upc.edu (V. Puig), cembrano@iri.upc.edu (G. Cembrano).

The control goal of autonomous driving system is to follow the references generated by the trajectory generator. This is a complicated task that must guarantee certain levels of performance and ensure vehicle stability. The trajectory-tracking problem is very crucial for autonomous racing vehicles, and many control algorithms have been proposed such as fuzzy controller [10], Linear Quadratic Regulator (LQR) [11], Model Predictive Control (MPC) [12] and Linear Parameter Varying (LPV) [13]. The idea of controlling nonlinear systems such as autonomous driving system considering LPV models has been widely investigated in the literature [13,14]. The main advantage of LPV models is that allows solving nonlinear problems in a quasi-linear mode by embedding the model non-linearities inside model parameters that depend on some scheduling variables [15]. In [16], authors propose a model predictive path tracking controller according to the vehicle dynamics and actuators conditions in its path tracking. Though, the planned path might not be adequately tracked by the vehicle since the vehicle dynamics and its constraints are not included in path generation [17]. In [18], a tracking method for a mobile robot is presented, where the fuzzy predictive control is used to predict the position and the orientation of the robot. A path tracking scheme for the mobile robot based on neural predictive control is introduced in [19], where a multi-layer back propagation neural network is employed to model kinematics of the robot.

In general, the main objective of the autonomous racing is to make the lap in the shortest possible time while maintaining a smooth driving behavior. However, if the objective is the minimization of the lap time, the controller has to plan the trajectory on an adequately time horizon to avoid steering the vehicle outside the track [20]. In this area, there are some research such as in [21] that proposes an adaptive MPC approach for solving lane keeping problem. In [22], a real-time MPC control scheme is introduced that solves the racing problem and test it in miniature race cars. Also, the Learning MPC is proposed to provide a solution to the racing problem in [20]. To minimize the time in a circuit implies going as fast as possible without exceeding circuit limits. But, it also affects the energy consumption of the vehicle and a trade-off between these two objectives have received great interest in recent years, particularly in the area of car racing. Several studies solve this problem by using an optimal control technique, [23] and [22]. However, the considered control framework requires the use of safe energy mechanisms which still have not been considered in scientific literature. In this paper, we propose to develop a framework for optimal compromise between control and energy management increasing enlarging the autonomous operation of the vehicle.

The increasing requirement for considering the reliability and availability of autonomous vehicles has led to the improvement and integration of prognostics and health management (PHM) techniques with automated systems [24,25]. There are two stages in PHM, particularly, *prognostics* and *health management*. Prognostic is classified as the main process in maintenance strategies according to the remaining useful life of the equipment, which allow anticipating critical damages and reducing costs [26]. The remaining useful life (RUL) is defined as the remaining time that a component (or system) will be able to perform its expected operation. This time regularly depends on the ageing of the components and the operating conditions. RUL estimation is a key element in condition based maintenance, prognostics and health management. Generally, RUL is unknown and random, and as such it should be estimated from available information provided by health monitoring and condition modules [27]. Regularly, the energy source of an autonomous racing vehicle is based on a battery. Obtaining more information about battery lifetime behavior would allow developing more cost-effective and long-lasting batteries. The performance of the racing vehicle is progressively

reduced over time because of the battery ageing . The effect of ageing is characterized by losing power. This deterioration is caused by several factors such as high-rate cycling, overburden and overdischarge [28]. To avoid damages and decrease the ageing rate during the charge/discharge cycles of the battery, it is required to monitor the State of Charge (SoC). The SoC is the proportion of the possible charge, compared to the total charge available when the battery is fully charged at a specific time.

A recent summary of methods for battery diagnosis can be found in [29,30]. The battery RUL prediction and the uncertainty management by using the particle filter (PF) approach (applying the practical degradation model to create a state transition equation) are provided in [31]. An integrated method based on a mixture of Gaussian process model and PF for battery SoH estimation is presented in [32]. Using the model-based tracking approach is a general way to obtain suitable results [33]. The usage of Kalman filtering for monitoring the SoC was reported in a lot of studies, e.g.[34,35]. On the other hand, motion control actions are observed as a source of stress degradation such as [36, 37]. In [38] the authors proposed an approach to estimate RUL based on assuming a decisive relation between the degradation and the control input. To the knowledge of the authors, there is no control approach in the literature that considers the SoC and RUL of the battery of a racing vehicle. For this reason, in this work, we propose a health-aware control approach for a racing vehicle as a novel approach to solve the autonomous driving control problem and at the same time to maintain and minimize the consumption of the battery energy.

The main contribution of this paper is to provide a health-aware control design for a racing vehicle that generates an optimal path for the racing by optimizing the lap time and maximizing the RUL of the battery in the planner. The control design is divided into two layers (path planner and controller) with different time scales. The first layer included a path planner whose objective is to optimize the lap time and maximize the battery RUL to obtain the best trajectory under the constraints of the circuit. The second layer is focused on a controller gain with integral action for tracking the trajectory obtained by the planner. Both optimization problems are solved using Linear Matrix Inequality (LMI) approach for MPC considering an LPV model of the vehicle and the input and output constraints. Several reasons justify the use of LMIs [39]. In fact, the resulting LMI-based optimization problems can be solved in polynomial time, using interior-point methods and the optimal solution is global [40]. Finally, the proposed approach is assessed in simulation and results show the effectiveness of the proposed planner for optimizing the lap time while at the same maximizing the RUL of the battery.

The remainder of the paper is organized as follows. In Section 2, the model of racing vehicle is introduced and the LPV model of vehicle is presented. The problem statement and the main control goal are presented in Section 3. The on-line optimization approaches for planner based on robust LMI control design including the battery health management is provided in Section 4. Moreover, the optimization approaches for controller to track the path of planner is introduced in Section 4. In Section 5, results of applying the proposed control strategy to a racing vehicle are summarized. In Section 6, the conclusions of this work are drawn and some research lines for future work are proposed.

Notation

Throughout this paper, $\mathbb{R}, \mathbb{R}_+, \mathbb{R}^n, \mathbb{R}^{m \times n}$ indicate the field of real numbers, the set of non-negative real numbers, the set of column real vectors of length n and the set of m by n real matrices, respectively. Define the set $\mathbb{I}_{[a,b]} := \{x \in \mathbb{I}_+ | a \leq x \leq b\}$ for some $a, b \in \mathbb{I}_+$ and $\mathbb{I}_{\geq c} := \{x \in \mathbb{I}_+ | x \geq c\}$ for some $c \in$

$\mathbb{I}_+$. The operator $\otimes$ is means the tensor product of two values. Furthermore, $\|.\|$ denotes the spectral norm for matrices and $\|.\|_2$ is the squared 2-norm symbol. The superscript $^\top$ represents the transpose and operators $<, \leq, =, >, \geq$ indicate element-wise relations of vectors.

2. System description and modeling

In racing, the race car drivers goal is to win a race, which means finishing the race with the smallest time. A race car driver has to drive the car as fast as possible without losing control of the vehicle at the limits. Moreover, it has to keep and control consistently the energy of the vehicle for keeping in the race. Therefore, a racing controller has to robustly track the desired path and stabilize the vehicle. For obtaining an optimal response in terms of maneuverability, it is required the vehicle to work in the dynamic limits established. The dynamic model of the vehicle used in this paper is a standard bicycle model version obtained from [41] described by means of the following equations

$$\dot{v}_x = \alpha + \frac{-F_{yf}\sin(\delta) - \mu m\,g}{m} + \omega v_y,$$
$$\dot{v}_y = \frac{F_{yf}\cos(\delta) + F_{yr}}{m} - \omega v_x, \tag{1}$$
$$\dot{\omega} = \frac{F_{yf}l_f\cos(\delta) - F_{yr}l_r}{I},$$

where v_x, v_y and ω are the body frame velocities linear in x, linear in y in (m/s) and angular velocity in (rad/s), respectively. δ is the steering angle in (rad) and α is longitudinal acceleration in (m/s^2), while both of them are control inputs of the system (see Fig. 1).

Moreover, F_{yf} and F_{yr} are the lateral forces produced in front and rear tires in (N), respectively, given by

$$F_{yf} = C_f\left(\delta - \frac{v_y}{v_x} - \frac{l_f\omega}{v_x}\right), \tag{2}$$
$$F_{yr} = C_r\left(-\frac{v_y}{v_x} - \frac{l_r\omega}{v_x}\right). \tag{3}$$

where variables C_f and C_r are the tire stiffness coefficient for the front and rear wheels. m and I represent the vehicle mass and inertia. l_f and l_r are the distances from the center of gravity to the front and rear wheel axes, respectively. μ and g are the friction coefficient and the gravity value, respectively.

On the other hand, the kinematic model is based on the velocity vector movement in order to obtain longitudinal and lateral velocities referenced to a global inertial frame [13]. Kinematic based model has generally used because its low parameter dependency. The kinematic model used in this paper is based on the error model which is obtained as the difference between the real position orientation states and their references. These kinematic equations are determined by the following curvature-based equations:

$$\dot{e}_y = \sin(e_\theta)v_x + \cos(e_\theta)v_y,$$
$$\dot{e}_\theta = \omega - \frac{\cos(e_\theta)v_x - \sin(e_\theta)v_y}{1 - e_y\kappa}\kappa, \tag{4}$$
$$\dot{s} = \frac{\cos(e_\theta)v_x - \sin(e_\theta)v_y}{1 - e_y\kappa},$$

where $\dot{e}_y$ and $\dot{e}_\theta$ are the heading lateral distance and angle error between the vehicle and the path and s indicates the distance traveled along the centerline of the road. κ is the circuit curvature and presents the lateral behavior reference. The vehicle model is concisely expressed in state space representation as
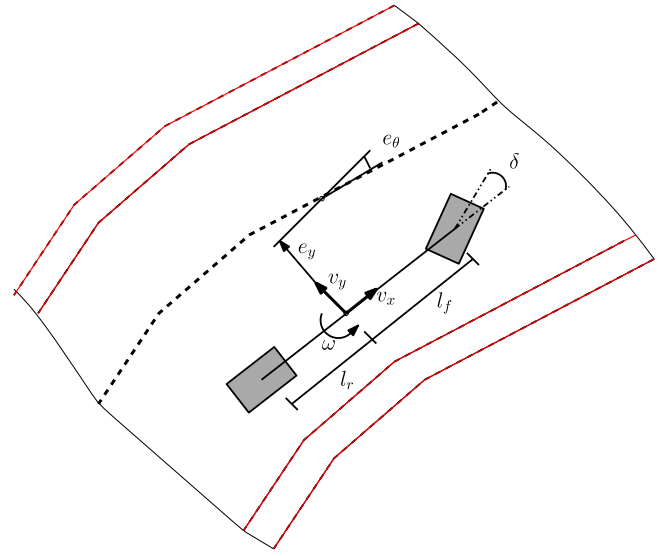
$$\dot{x}(t) = f(x(t), u(t), w(t), v(t)), \tag{5}$$

Fig. 1. Racing vehicle variables along the road.

where at time t the vectors x, u, w and v represent the state, input, disturbances and noise

$$x = [v_x\ v_y\ \omega\ e_y\ e_\theta]^\top, \quad u = [\delta\ \alpha]^\top, \tag{6}$$

and v is the measurement noise that is applied into measurable states and w is the friction force disturbances that is considered as a variation of the nominal friction force $F_{friction} = \mu mg$.

In order to achieve the best trajectory where the lap time is optimized, the time (t) should considered as a state variable. This is achieved by formulating kinematic model (4) in the space domain considering the time (t) as a state variable which will be used for optimizing the lap time. Furthermore, because of the problem consists on finding out the best path, the curvature (κ) has to be implemented in terms of the driven distance since the time evolution is unknown at the beginning of the optimization. By considering $x_c = [e_y,\ e_\theta,\ s]^\top$ as the state vector of kinematic model (4), then, a new state vector $\tilde{x}_c = [\tilde{e}_y,\ \tilde{e}_\theta,\ t]^\top$ is determined by applying

$$\tilde{x}_c = \frac{dx_c}{ds} = \frac{dx_c}{dt}\cdot\frac{dt}{ds} = \dot{x}_c\frac{1}{\dot{s}}. \tag{7}$$

Then, the following kinematic model equation when the time is considered as a state in the model

$$\tilde{e}_y = \sin(e_\theta)v_x + \cos(e_\theta)v_y,$$
$$\tilde{e}_\theta = \frac{\omega}{\dot{s}} - \kappa, \tag{8}$$
$$\tilde{t} = \frac{1}{\dot{s}}.$$

The main goal of this paper is to maximize the Remaining Useful Life (RUL) of the battery vehicle that has a direct connection by reducing vehicle energy consumption as low as possible considering that the energy is stored in the battery. In order to minimize the vehicle energy and maximize the RUL, the state of charge (SoC) of the battery must be considered as a state variable. The SoC of a battery at a given time is the proportion of the charge available, compared to the total charge available when it is fully charged. The range for the battery state of charge is defined as $SoC \in [0, 1]$, where 0 denotes the battery is fully discharge, and 1 corresponds to 100% of the charge, i.e., that, the battery is fully charged. Based on the previous study [35], the most common

used approach to compute the SoC is described as follows:

$$SoC(t) = SoC(t_0) - \frac{1}{C_T} \int_{t_0}^{t} I_{batt}(t)dt, \tag{9}$$

where t_0 presents the initial time and C_T is total capacity of the battery. However, to include the SoC of the battery in the vehicle model, the SoC can be expressed in function of the velocity of the vehicle. Then, the SoC in the battery can be modeled as follows

$$SoC(t) = SoC(t_0) - P_{batt}(t),$$
$$P_{batt}(t) = P_{move}(t) + P_{friction}(t), \tag{10}$$
$$P_{batt}(t) = \frac{1}{2}C_d \rho A_r v_x^2 + \mu mg v_x,$$

where C_d is drag coefficient for the wheel, A_r indicates the vehicle front area and ρ is the air density at 25°C.

Therefore, based on the (1)–(10), Eq. (5) can be expressed as:

$$\dot{\tilde{x}}(t) = \tilde{f}(\tilde{x}(t), u(t), w(t), v(t)), \tag{11}$$

where the augmented vector of states is defined as follows

$$\tilde{x}(t) = [v_x, \ v_y, \ \omega, \ \tilde{e}_y, \ \tilde{e}_\theta, \ t, \ SoC]^\top, \tag{12}$$

2.1. LPV Modeling

The previous vehicle non-linear model will be transformed into an LPV representation by embedding the nonlinearities inside some varying parameters following the procedure presented in [42]. As a result, these parameters are expressed in terms of some system variables called scheduling variables that vary in a known bounded interval. This procedure leads to the following LPV model in discrete-time

$$\tilde{x}(k+1) = A(\theta(k))\tilde{x}(k) + B(\theta(k))u(k) + Ew(k)$$
$$\tilde{y}(k) = C\tilde{x}(k) + Dv(k), \tag{13}$$

where the $k \in \mathbb{N}$ is the discrete time instant. The matrices A, B, C and E are as follows

$$A(\theta(k)) = \begin{bmatrix} a_{11} & a_{12} & a_{13} & 0 & 0 & 0 & 0 \\ 0 & a_{22} & a_{23} & 0 & 0 & 0 & 0 \\ 0 & a_{32} & a_{33} & 0 & 0 & 0 & 0 \\ 0 & 1 & 0 & 0 & a_{45} & 0 & 0 \\ 0 & a_{52} & a_{53} & 0 & 1 & 0 & 0 \\ a_{61} & a_{62} & 0 & 0 & 0 & 0 & 0 \\ a_{71} & 0 & 0 & 0 & 0 & 0 & 1 \end{bmatrix},$$

$$B(\theta(k)) = \begin{bmatrix} b_{11} & 1 \\ b_{21} & 0 \\ b_{31} & 0 \\ 0 & 0 \\ 0 & 0 \\ 0 & 0 \\ 0 & 0 \end{bmatrix}, \ E = \begin{bmatrix} 1/m \\ 0 \\ 0 \\ 0 \\ 0 \\ 0 \\ 0 \end{bmatrix},$$

$$C = \begin{bmatrix} 1 & 0 & 0 & 0 & 0 & 0 \\ 0 & 1 & 0 & 0 & 0 & 0 \\ 0 & 0 & 1 & 0 & 0 & 0 \end{bmatrix}.$$

The mathematical expressions of the varying parameters in matrices A and B are provided in Appendix. The vector $\theta(k) \in \mathbb{R}^{n_\theta}$ is the vector of varying parameters. Each parameter θ_j varies in a defined interval $\theta_j \in [\underline{\theta_j}, \overline{\theta_j}] \ \forall j \in [1, \ldots, n_\theta]$, which belongs to a convex polytope Θ defined by

$$\Theta := \left\{ \theta(k) \in \mathbb{R}^{n_\theta} \ \middle| \ \sum_{j=1}^{N} \mu_j(\theta(k)) = 1, \ \mu_j(\theta(k)) \geq 0 \right\}, \tag{14}$$

where $N = 2^{n_\theta}$ is the number of vertices models obtained from the vertices of the polytope (14). The coefficients μ_j of the polytopic decomposition are given by

$$\mu_j(\theta(k)) = \prod_{j=1}^{N} \zeta(\eta_0^j, \eta_1^j),$$
$$\eta_0^j = \frac{\overline{\theta_j} - \theta_j}{\overline{\theta_j} - \underline{\theta_j}}, \quad \eta_1^j = 1 - \eta_0^j. \tag{15}$$

Clearly, as $\theta(k)$ varies inside the convex polytope Θ, the matrices of the system (13) vary inside a corresponding polytope Ψ, which is defined by the convex hull (Co) of N matrix vertices $[A_j, B_j, E, C, D], j \in [1, \ldots, N]$,

$$\Psi := Co \left\{ \begin{bmatrix} A_1 & B_1 & E & C & D \end{bmatrix}, \begin{bmatrix} A_2 & B_2 & E & C & D \end{bmatrix}, \ldots, \begin{bmatrix} A_N & B_N & E & C & D \end{bmatrix} \right\}, \tag{16}$$

Using the matrices (16), the system (13) can be rewritten in polytopic form as follows

$$A(\theta(k)) = \sum_{j=1}^{N} \mu_j(\theta(k))A_j, \quad B(\theta(k)) = \sum_{j=1}^{N} \mu_j B_j(\theta(k)). \tag{17}$$

3. Problem statement

The main control goal for the vehicle is to obtain the best path trajectory according to the vehicle dynamics and its limits for racing. Then, the controller forces the vehicle to track the trajectory obtained online by the planner. However, if the objective is only the minimization of the lap time, the controller has to plan the trajectory on an adequately time horizon to avoid steering the vehicle outside the track. But, this plan also affects the energy consumption of the vehicle. Thus, the management of the trade-off between these two objectives is an open problem in the area of car racing. Therefore, in addition to obtaining a planned trajectory with optimal lap time, the energy consumption of the vehicle that depends on the battery RUL should be considered into the optimization problem solved by the planner.

Generally, the design of multi-layer control structures can be related to the different type of control objectives, which would not be able to be addressed considering a single layer architecture [43]. Specifically, the control objectives can be arranged in the following way:

- The objectives of planner operation are to minimize lap time and maximize battery lifetime. Since, the assessing the battery SoC requires more time than the tracking trajectory evaluation, the planner operates at slowly time scale that the controller.
- The objectives of controller are to guarantee a stable operation of the vehicle while tracking the trajectory provided by the planner.

The control strategy presented in this paper is based on a multilayer (hierarchicalcontrol structure including the energy management. This structure, conceptualized in Fig. 2, is a two-layer hierarchical architecture, where the solution of the problem is obtained by decoupling the problem into two different time-scales. In the upper layer, the planner solves an optimization problem that has a objective to provide the optimal path (references that are shown by subindex r in Fig. 2) to the automatic control (low layer). In the lower layer, the tracking controller receives the path trajectory calculated by the upper layer and determines the best trajectories for the controller-layer, which is operated by pole placement method, by considering the faster dynamics of the plant.
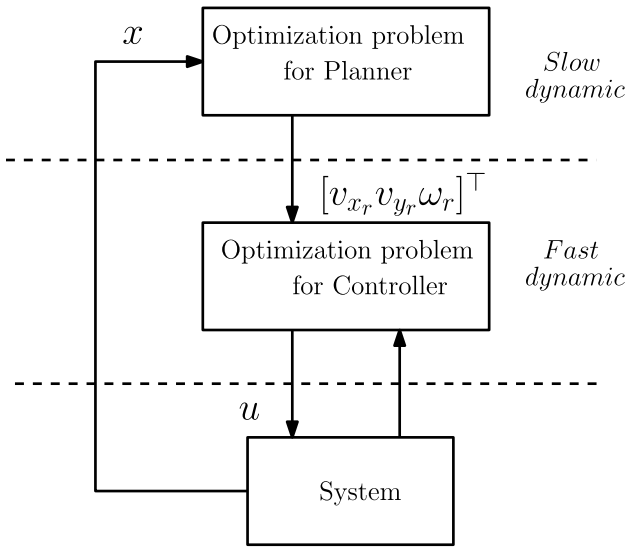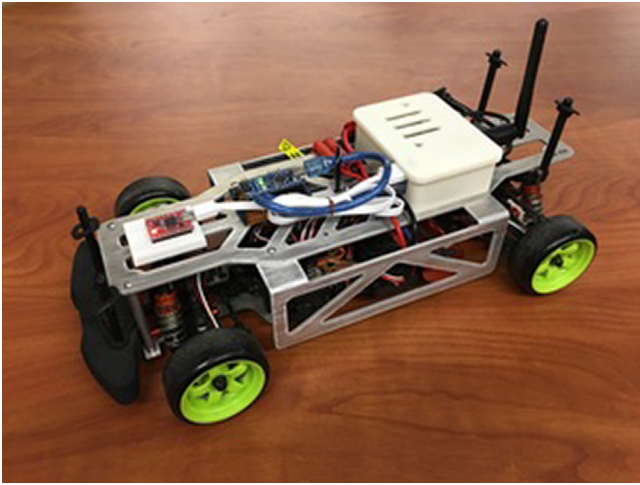
Fig. 2. Block diagram of control approach.

Fig. 3. Berkeley Autonomous Vehicle [44]. .

4. Proposed approach

4.1. LPV MPC Planner

The main goal of the planner part is to find the optimal path within the circuit and provide such information to the controller. In general, the path trajectory is obtained according to the body frame velocities of the vehicle. In this paper, for solving these optimization problems to obtain the best path, a robust LMI-based MPC controller, which is able to deal with the unknown future evolution of the varying parameters of the LPV model in the prediction horizon, is considered. This approach consider that the varying parameters in this horizon are not exactly known but instead are considered to vary inside the corresponding regions of variation determined by the operational limits of the scheduling variables. Hence, the optimal control problem can be reformulated as the following robust LMI-based MPC [45], which minimizes the infinite horizon quadratic objective function:

$$J_\infty(k) = \sum_{i=0}^{\infty}(\| \tilde{x}(k + i|k) \|_{Q_1} + \| \tilde{u}(k + i|k) \|_R), \tag{18}$$

where $\tilde{u} = [\delta\ \alpha]^\top$ is the control input generated by the planner. Moreover, $\tilde{x}(k + i|k)$ and $\tilde{u}(k + i|k)$ denote the state predicted based on the measurements and the control input at time $k + i$, computed at time k, respectively. $\tilde{x}(k) = \tilde{x}(k|k)$ and $\tilde{u}(k) = \tilde{u}(k|k)$ denote the measured state and control input planned for time k, respectively. Besides, $Q_1 = Q_1^\top > 0$ and $R^\top > 0$ are positive definite weighting matrices.

The control law is obtained by minimizing cost function (18) with respect to the control moves, that is:

$$\min_{\tilde{u}(k+i|k),i\geq0}\ \max_{[A(k+i),B(k+i)]\in\Psi,i\geq0} J_\infty(k), \tag{19}$$

where the maximization in (19) is taken over the set Ψ of the polytopic representation of the LPV model (16). The solution of (19) leads to a state feedback law for planner given by:

$$\tilde{u}(k + i|k) = K(\theta(k))\tilde{x}(k + i|k), \tag{20}$$

where the state feedback gain is given by

$$K(\theta(k)) = \sum_{j=1}^{N} \mu_j(\theta(k))K_j, \tag{21}$$

which optimizes (19).

4.2. LMI Control design of planner including health management

One of the motivations in this work is to integrate the information about the battery SoC in the planner and controller design. Accordingly, the battery lifetime will be estimated by means of the RUL computed using an approach based on the SoC.

4.2.1. RUL computation via SoC assessment
Once the battery SoC is calculated for the racing vehicle, an approach to evaluate RUL function is introduced.

Proposition 1. *Considering that RUL is computed when the state of charge behavior reaches (or exceed) the state of charge threshold value which is denoted by SoC_{thresh}. Therefore, the expected RUL is given by*

$$RUL(k) = \frac{SoC_{thresh} - SoC(k)}{-u_b(k)}, \tag{22}$$

where u_b is the battery input.

Proof. The derivative of the state of charge of the battery is given by

$$\frac{d(SoC)}{dt} = u_{discharge}(k), \tag{23}$$

or, equivalently in discrete-time can be rewritten as follows

$$\frac{SoC(k + 1) - SoC(k)}{\Delta t} = u_{discharge}(k). \tag{24}$$

Assuming the $SoC(k + 1)$ reaches the SoC threshold (SoC_{thresh}), where SoC threshold is the point at which the battery would no longer reliably provide energy for moving the vehicle. Then, (24) can be rewritten as:

$$\frac{SoC_{tresh} - SoC(k)}{\Delta t} = u_{discharge}(k) \tag{25}$$

According to (25), the definition of the RUL and considering that δt provides an estimation of the RUL yields to:

$$RUL(k) = \frac{SoC_{thresh} - SoC(k)}{u_{discharge}(k)}, \tag{26}$$

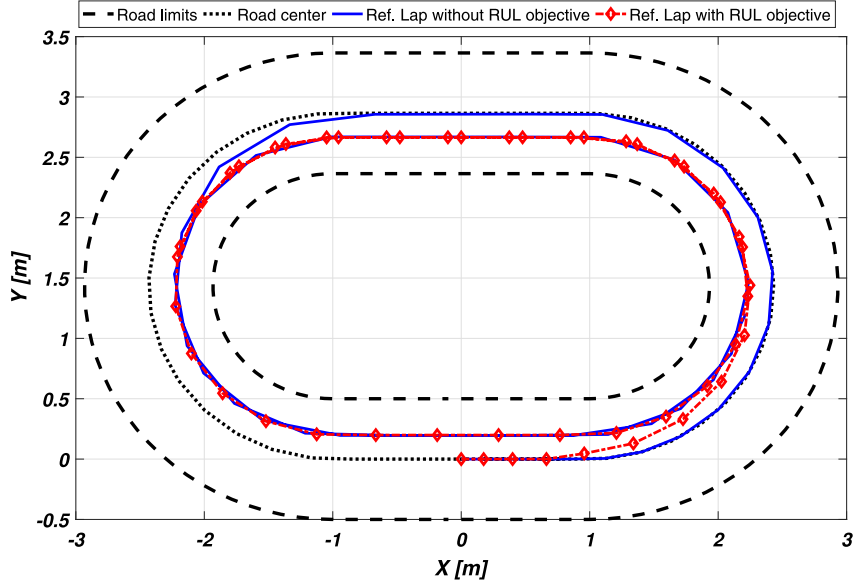where, $u_{discharge}$ is considered the negative value of the battery input that is denoted by $-u_b$.

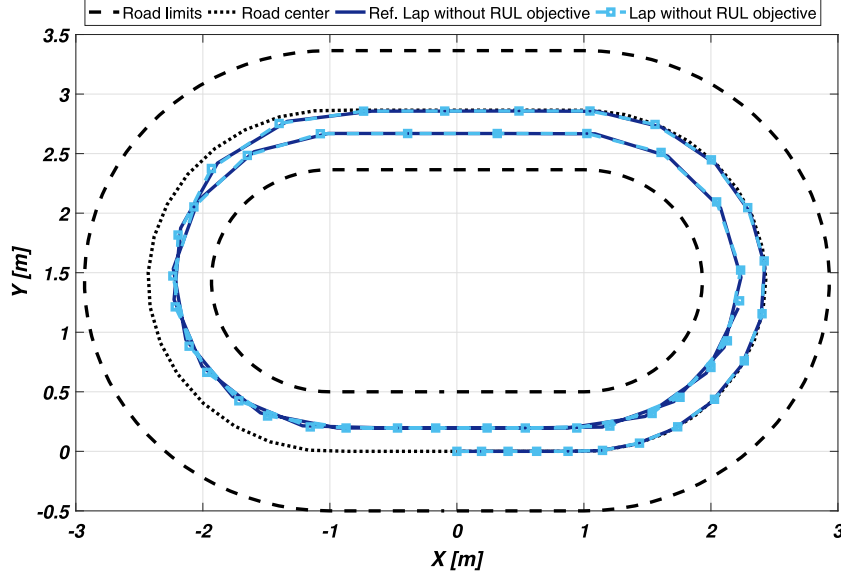**Fig. 4.** Comparison of planner racing laps with and without RUL objective.

Fig. 5. The reference and response of racing lap without RUL objective.

4.2.2. LMI Control design based RUL objective

The LMI control design for the planner based on the optimizing the lap time and RUL objectives is now proposed for the racing vehicle. The objective of the trajectory planner is modified to find the best path within the circuit that optimizes the lap time t and at the same time maximizes the lifetime of the battery. In order to increase the RUL of the battery and optimizing the lap time, the optimization planner objective (18) should be modified according to the new objective. According to the (22), there is a relation between the RUL and battery SoC and control input. Moreover, the SoC model (8) and (10) are considered as new states in the vehicle model. Hence, the optimization planner can be updated based on the RUL and lap time and the robust LMI optimization problem of the planner (18) is reformulated as follows:

$$\min_{\tilde{u}(k+i|k),i\geq0} \max_{[A(k+i),B(k+i)]\in\Psi,i\geq0} J_{g,\infty}(k) = \sum_{i=0}^{\infty}(\parallel t \parallel^2_{\lambda_1} + \parallel \frac{1}{RUL} \parallel^2_{\lambda_2}),$$

(27)

where λ_1 and λ_2 are positive definite weighting matrices, that allow establishing the trade-off between lap time and battery RUL.

Given that the time t is considered as an additional state of the model and the RUL is estimated based on the SoC which is another state of the model, the optimization problem (27) can be solved as a LQR problem based on the robust LMI similarly to (18). Therefore, the state feedback control law now can be formulated for the LPV planner model as follows:

$$\tilde{u}(k+i|k) = K_g(\theta(k))\tilde{x}(k+i|k),$$

(28)

where the state feedback gain matrix is given by

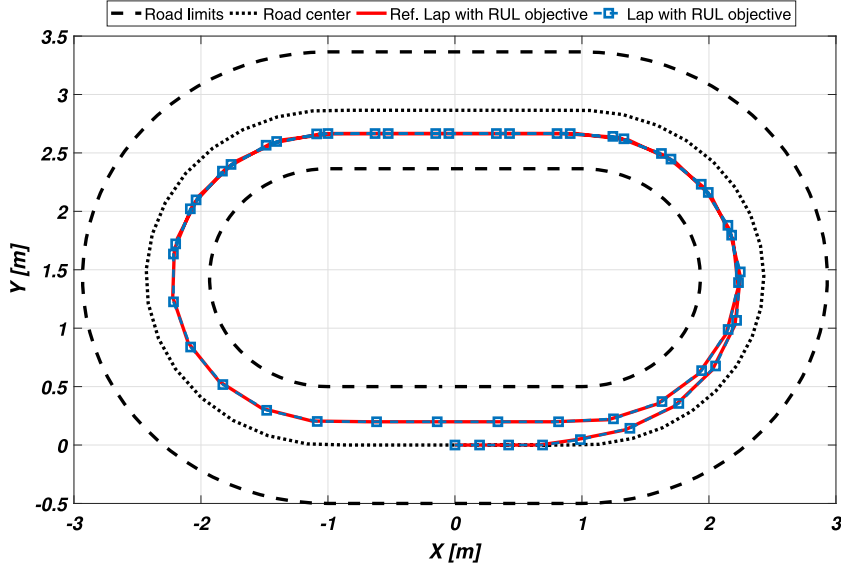$$K_g(\theta(k)) = \sum_{j=1}^{N} \mu_j(\theta(k))K_j,$$

(29)

Fig. 6. The reference and response of racing lap with RUL objective.
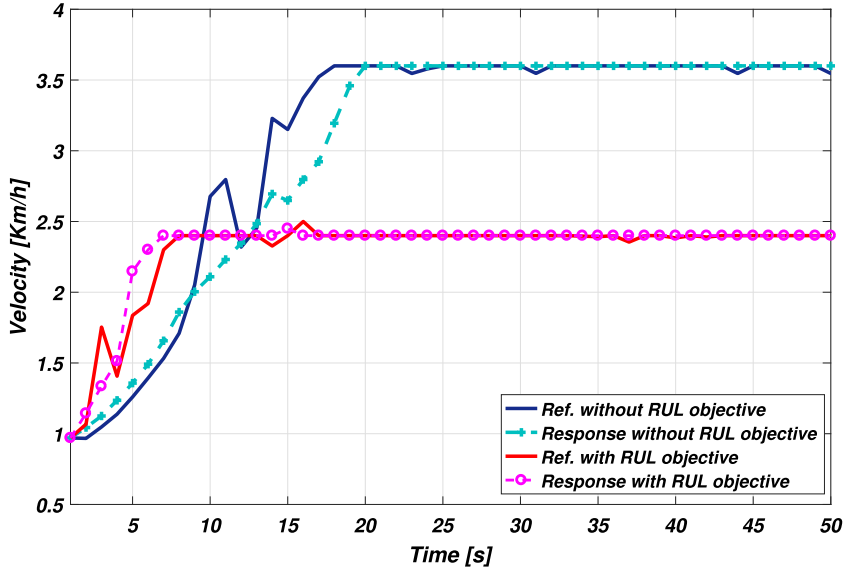

Fig. 7. Comparison of the velocity with and without the RUL objective.

that is obtained using a theorem that will be introduced in the following based on the [45], but adapted to the racing vehicle and using the new objective function (27). Before presenting the theorem, let consider some auxiliary lemmas.

Lemma 1 ([46]). *Consider A as a symmetric matrix. Then*

$$\lambda_{max}(A) \leq 0 \iff \gamma A - \gamma I \leq 0. \tag{30}$$

Lemma 2 ([46]). *Consider A a matrix of appropriate dimensions, and γ a positive scalar. Hence,*

$$A^\top A - \gamma^2 I \leq 0 \iff \begin{bmatrix} -\gamma I & A \\ A^\top & -\gamma I \end{bmatrix} \leq 0. \tag{31}$$

Lemma 3 (*Schur Complement Lemma*). *[46] Consider*

$$\begin{bmatrix} Q(x) & S(x) \\ S^\top(x) & R(x) \end{bmatrix} > 0, \tag{32}$$

where $Q(x) = Q^\top(x)$, $R(x) = R^\top(x)$ and $S(x)$ is the affine function of x. Then, (32) is equivalent to the following conditions:

$$Q(x) > 0, \quad R(x) - S^\top(x)Q^{-1}(x)S(x) > 0,$$
$$R(x) > 0, \quad Q(x) - S(x)R^{-1}(x)S^\top(x) > 0. \tag{33}$$

Theorem 1. *Considering $\tilde{x}(k|k)$ is the state of the system (13) measured at each sampling time k and that there are constraints on the output and control input where u_{max} and $\tilde{y}_{max}$ are the maximum values of control input and output of vehicle. The state feedback matrix K in the control law $\tilde{u}(k + i|k) = K_g(\theta(k))\tilde{x}(k + i|k)$ that minimizes the upper bound on the performance objective function at sampling time k_g given by $K_g = YQ^{-1}$ can be found, if there exist K_g, Q, γ and $\gamma \in \mathbb{R}^{1\times1} > 0$, $Q = Q^\top \in \mathbb{R}^{7\times7} > 0$, $Y \in \mathbb{R}^{2\times7}$ where Q and Y are obtained from the solution of the following linear objective minimization problem*
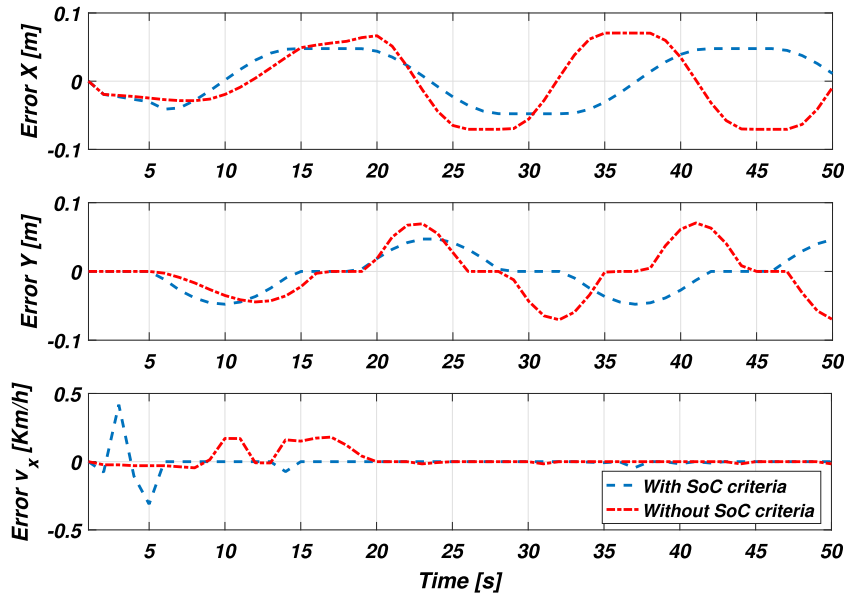
$$\min_{\gamma,Q,Y} \gamma \tag{34}$$

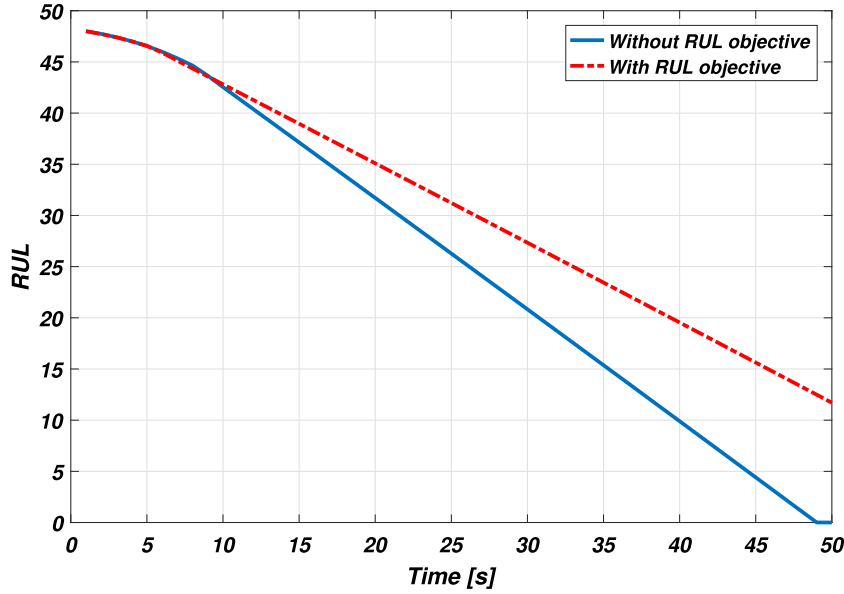**Fig. 8.** Error achieved during the simulation racing laps.

Fig. 9. Comparison of the battery RUL.

$$\begin{bmatrix} 1 & \tilde{x}(k)^\top \\ \tilde{x}(k) & Q \end{bmatrix} \geq 0, \tag{35}$$

$$\begin{bmatrix} Q & * & * & * \\ A_j Q + B_j Y & Q & 0 & 0 \\ Q_1^{1/2} Q & 0 & \gamma I & 0 \\ R^{1/2} Y & 0 & 0 & \gamma I \end{bmatrix} > 0, \tag{36}$$

$$\begin{bmatrix} -\gamma I & (-1/RUL(k)) \\ (-1/RUL(k))^\top & -\gamma I \end{bmatrix} \leq 0, \tag{37}$$

$$\begin{bmatrix} u_{max}^2 I & Y \\ Y^\top & Q \end{bmatrix} \geq 0, \tag{38}$$

$$\begin{bmatrix} Q & (A_j Q + B_j Y)^\top C^\top \\ C(A_j Q + B_j Y) & \tilde{y}_{max}^2 \end{bmatrix} \geq 0, \tag{39}$$

Proof. The proof is obtained applying the following steps:

(1) Proof for the stability and optimization.

By considering a quadratic Lyapunov–Krasovskii function $V(x(k)) = \tilde{x}^\top(k) P \tilde{x}(k) > 0$, where $P > 0$ is a symmetrical positive-definite matrix, the upper bound on the objective function J_∞ is obtained.

To guarantee the existence of the upper bound on the performance at sampling time k, the following inequalities must be satisfied

$$V(\tilde{x}(k+i+1|k)) - V(\tilde{x}(k+i|k)) \leq -J_{g,\infty}(k)$$
$$\forall [A(k+i), B(k+i)] \in \Psi, i \geq 0 \tag{40}$$

Then, by requiring $\tilde{x}(\infty|k) = 0$ such that $V(\tilde{x}(\infty|k)) = 0$ and summing (40) from $i = 0$ to $i = \infty$, it can be obtained

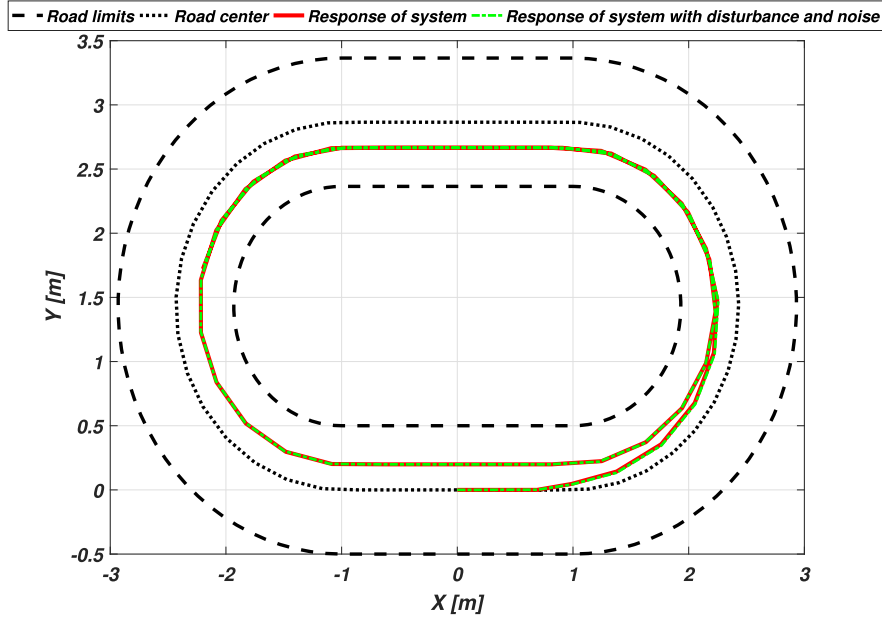$$\max_{[A(k+i),B(k+i)] \in \Psi, i \geq 0} J_\infty \leq V(\tilde{x}(k|k)). \tag{41}$$

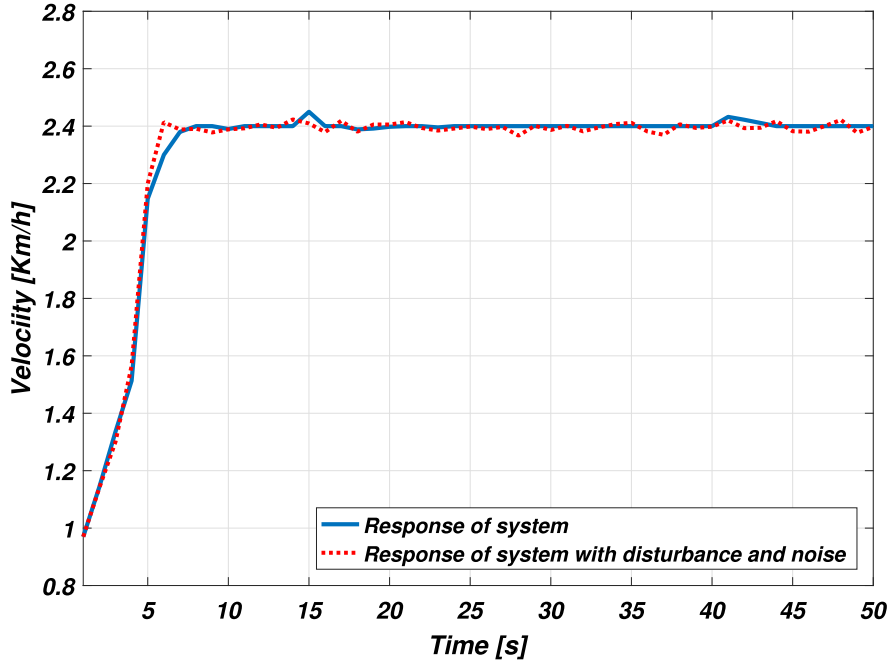**Fig. 10.** Comparison of the Response with and without the disturbance and noise with RUL objective.

Fig. 11. Comparison of the velocity with and without the disturbance and noise with RUL objective.

The minimization of $V(\tilde{x}(k)) = \tilde{x}(k)^\top P\tilde{x}(k)$ (with $P > 0$) is equivalent to

$$\min_{\gamma, P} \gamma$$

s.t. $\tilde{x}(k)^\top P\tilde{x}(k) \leq 0.$

Defining $Q = \gamma P^{-1} > 0$ and using the Schur-complement [46], the (35) is established.

Then, by substituting (13) and (28), inequality (40) becomes:

$$\tilde{x}(k+i|k)^\top \left((A(k+i) + B(k+i)K_g)^\top P(A(k+i) + B(k+i)K_g) - P \right.$$
$$\left. + K_g^\top RK_g + Q_1 \right) \tilde{x}(k+i|k) \leq 0.$$

that it is defined in $[A(k+i), B(k+i)]$. Then, it is satisfied for all $[A(k+i), B(k+i)] \in \Psi$. Hence, by substituting $P = \gamma Q^{-1}$, $Q > 0$, $Y = K_g Q$, pre - and post-multiplying by Q and using Lemma 3, (36) is obtained.

(2) Proof for maximizing the RUL of battery. According to objective (27) and definition of $\| (1/RUL) \|^2$, we have

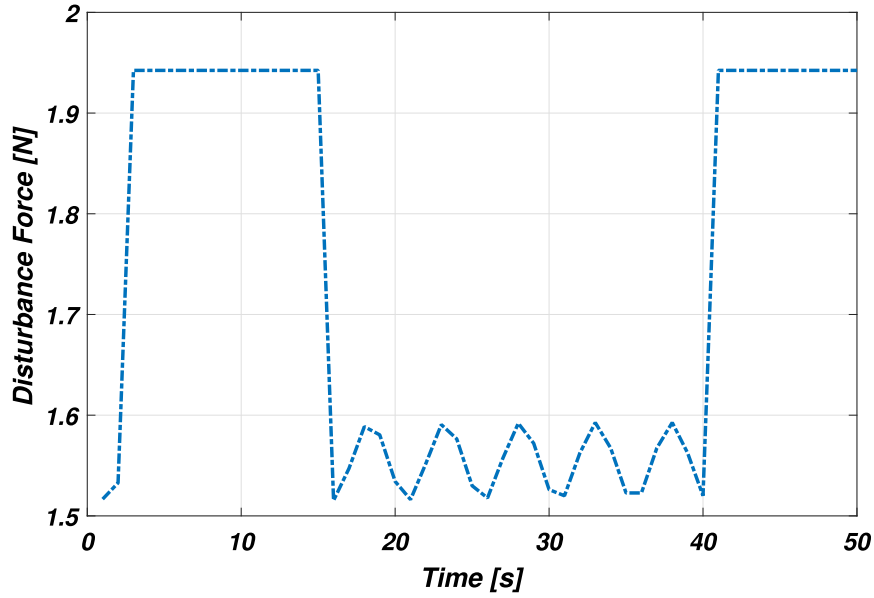$$\| (1/RUL) \|^2 = (\lambda_{max}((1/RUL)^\top (1/RUL)))^{\frac{1}{2}}.$$

Fig. 12. Friction force disturbance.

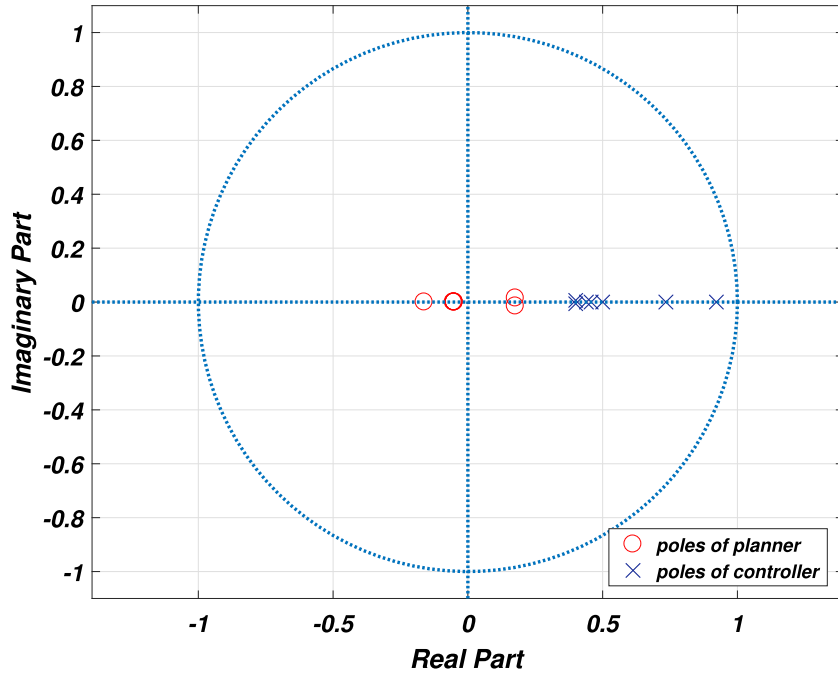**Fig. 13.** Poles positions of the planner and controller in a particular operating point.

Then, by using Lemmas 1 and 2, for $\gamma > 0$

$$\| (1/RUL) \|^2 \leq \gamma$$
$$\iff \lambda_{max}((1/RUL)^\top (1/RUL)) \leq \gamma^2,$$
$$\iff (1/RUL)^\top (1/RUL) - \gamma^2 \leq 0,$$
$$\iff \begin{bmatrix} -\gamma I & (-1/RUL(k)) \\ (-1/RUL(k))^\top & -\gamma I \end{bmatrix} \leq 0.$$

(3) Inclusion of output and input constraints.

Consider the Euclidean norm bound and maximum bound on the constraints of input

$$\|\tilde{u}(k + i|k)\|_2 \leq u_{max}.$$

Following [45],

$$V(\tilde{x}(k + i|k)) = \tilde{x}(k + i|k)^\top Q^{-1} \tilde{x}(k + i|k)$$
$$\leq \tilde{x}(k|k)^\top Q^{-1} \tilde{x}(k|k) \leq 1,$$

(42)

is state-invariant ellipsoid. Therefore, it can be obtained

$$\max_{i \geq 0} \|\tilde{u}(i|k)\|_2^2 = \max_{i \geq 0} \|YQ^{-1}\tilde{x}(i|k)\|_2^2$$
$$\leq \lambda_{max}(Q^{-1/2} Y^\top Y Q^{-1/2}) \geq u_{max}^2$$

where λ_{max} denotes the largest generalized eigenvalue and by using Lemma 3, (38) is obtained.

The output constraints (39) are satisfied based on the

$$\|y(k+i|k)\|_2 \leq y_{max}.$$

Thus,

$$\max_{i \geq 1} \ \|y(i|k)\|_2 = \max_{i \geq 0} \ \|[C \ 0](A_g + B_g K_g)\tilde{x}(i|k)\|_2$$
$$\leq \lambda_{max}([C \ 0](A_g + B_g K_g)Q^{1/2}) \leq y_{max}$$

Then, by multiplying on the left and right by $Q^{1/2}$

$$Q^{1/2}((A_g + B_g K_g)[C \ 0]^\top [C \ 0](A_g + B_g K_g))Q^{1/2} \leq y_{max}^2 I$$

such that by using Lemma 3, the inequality (39) is satisfied.

4.3. Tracking controller

The controller objective is to track the reference that is generated by the planner considering the same constraints on inputs and states. The controller is designed by pole placement and augmenting the plant with an integrator to remove steady state errors. The integrator can be including the following equation in the state space model of the vehicle

$$z(k+1) = z(k) + (y_r(k) - C\tilde{x}(k)), \tag{45}$$

where y_r is the references that are obtained by the planner. Thus, the augmented vehicle model (13) with integrator is

$$\begin{bmatrix} \tilde{x}(k+1) \\ z(k+1) \end{bmatrix} = \begin{bmatrix} A(\theta(k)) & 0 \\ -T_s C & I \end{bmatrix} \begin{bmatrix} \tilde{x}(k) \\ z(k) \end{bmatrix} + \begin{bmatrix} B(\theta(k)) \\ 0 \end{bmatrix} u(k)$$
$$+ \begin{bmatrix} 0 \\ T_s I \end{bmatrix} y_r(k) + \begin{bmatrix} E \\ 0 \end{bmatrix} w(k) \tag{46}$$
$$y(k) = \begin{bmatrix} C & 0 \end{bmatrix} \begin{bmatrix} \tilde{x}(k) \\ z(k) \end{bmatrix}$$

Then, the feedback control law can be formulated as follows using state feedback

$$u(k) = [K_c(\theta(k))] \begin{bmatrix} \tilde{x}(k) \\ z(k) \end{bmatrix}, \tag{47}$$

where $K_c = [K_{c1} K_{c2}]$ is the feedback gain matrix obtained using the LMI based formulation for solving the LPV LQR problem via an H_2 problem [13].

For obtaining a faster dynamics in the lower layer than in the upper layer, the position of poles should be forced close to the zero and inside the unit circle region. The stability and location of poles in the lower layer controller $\mathcal{D}$-stability concept is used. By using the definition of the $\mathcal{D}$-stability based on the region and [47], which is a subset $\mathcal{D}$ of the complex plane determined for a symmetric matrix $a = [a_{kl}] \in \mathbb{R}^{m \times m}$ and a matrix $b = [b_{kl}] \in \mathbb{R}^{m \times m}$such that:

$$\mathcal{D} = \{g \in \mathbf{C} : f_D(g) < 0\},$$

where $f_D(g)$ is the characteristic function, defined as follows

$$f_D(g) = a + gb + g^* b = [a_{kl} + gb_{kl} + g^* b_{kl}]_{1 \leq k,l \leq m} \tag{48}$$

and g^* denotes the complex conjugate of g.

By considering the closed-loop model $\mathcal{M}$, the controller gain $K_j h$ is designed such that

$$\mathcal{M} = \{(A_j + B_j K_j) : eig \ (A_j + B_j K_j) \in \mathcal{D}\}. \tag{49}$$

Therefore, by following the [47], the closed-loop system is quadratically $\mathcal{D}$-stable if there exists a symmetric matrix $P > 0$ such that:

$$a \otimes P + b \otimes (A_j + B_j K_j)P + b^\top \otimes ((A_j + B_j K_j)P)^\top < 0, \tag{50}$$

Table 1
Model parameters value.

Parameter	Value	unit
l_f	0.125	m
l_r	0.125	m
C_f	68	N/rad
C_r	71	N/rad
C_d	0.36	N/rad
I	0.03	kg/m^2
m	1.98	kg
μ	0.5	N/rad
ρ	1.184	kg/m^3
A_r	1.91	m^2

then, by substituting $W_j = K_j P$ and establishing that all the poles of closed-loop system should be inside the circular region centered in $(q, 0)$ with radius r, it can be shown that:

$$\begin{bmatrix} -rP & qP + A_j P + B_j W_j \\ qP + PA_j^\top + W_j^\top B_j^\top & -rP \end{bmatrix} < 0. \tag{51}$$

Therefore, by considering (51) and the dimensions of the system (12), the following proposition based on [46] can be modified considering the vehicle LPV model.

Proposition 2 ([39]). *Given the LQR parameters $Q = Q^\top \in \mathbb{R}^{7 \times 7} > 0$, $Y \in \mathbb{R}^{2 \times 7}$, a state feedback control in the form of $u(k) = K_c(\theta(k))[\tilde{x}(k), z(k)]^\top$ exists such that $\gamma > 0$, if and only if there exist $P \in \mathbb{R}^{7 \times 7}$, $Y \in \mathbb{R}^{2 \times 2}$ and $W_j \in \mathbb{R}^{2 \times 7}$ satisfying*

$$(A_j P + B_j W_j) + (A_j P + B_j W_j)^\top + \tilde{x}_0 \tilde{x}_0^\top < 0, \tag{52}$$

$$trace\left(Q^{1/2}X(Q^{1/2})^\top \right) + trace(Y) < \gamma, \tag{53}$$

$$\begin{bmatrix} -Y & R^{1/2}W_j \\ (R^{1/2}W_j)^\top & -P \end{bmatrix} < 0, \tag{54}$$

$$\begin{bmatrix} -rP & qP + A_j P + B_j W_j \\ qP + PA_j^\top + W_j^\top B_j^\top & -rP \end{bmatrix} < 0. \tag{55}$$

where a feedback gain is given by $K_{c,j} = W_j P^{-1}$.

Remark 1. It is important to note that the optimal solution from the planner in online mode may fail to exist. For such cases, the planner and controller optimization problems are solved separately. It means that the robust LMI problem is solved by an optimal offline trajectory planner that calculates the best trajectory under the constraints of the circuit. Then, the controller part using that trajectory as references for tracking the best path under the same constraints.

5. Simulation results

The performance of the proposed approach that utilizes a planner that includes battery energy management and tracking controller are assessed with a case study based on the Berkeley autonomous racing vehicle that is shown in Fig. 3. This vehicle can be modeled using the non-linear model (1)-(3) with the parameters presented in Table 1.

An *oval* circuit is chosen for assessing the proposed strategy that endeavors to cover various driving conditions as acceleration platforms and speed loss on curves also driving on different road situations. Therefore, there exist the unknown friction forces related to the different situations which are considered as disturbances. According to the different velocity and circuit shape, a trajectory planner has responsibility for creating a feasible trajectory

by using a polynomial curve production method [44]. In addition, computing consecutive and differentiable curves (accelerations and velocities) under an overall constrained vehicle acceleration are consisted. Hence, in an on-line mode, the planner algorithm including the health management creates the linear and angular velocity references plus requested positions and orientations for the control loop.

Based on *oval* circuit, the robust LMI-based optimization problem for planner is solved by using Theorem 1 for obtaining the best trajectory, where the objective is to minimize the lap time and at the same time maximizing the RUL of the battery. The battery RUL is computed by using Proposition 1. To compute (22), the mean value of interval longitudinal acceleration ($\underline{\alpha}$, $\overline{\alpha}$) is considered. The planner tuning is based on finding a best trade-off between maximizing the battery RUL and minimizing lap time by properly selecting the weights λ_1 and λ_2 in the objective function (27).

The trajectory path that obtained by the planner according to the *oval* circuit shape with and without considering maximization of the RUL objective (37) inside the robust LMI problem of planner are presented in Fig. 4. From Fig. 4, it can observed that the racing trajectory of the planner in the case of the RUL objective that shows by diamond dash line, after some iteration goes to close to the lower bound of the circuit for saving the energy of battery. However, the trajectory path of the planner in the case of without the RUL objective that shows straight line after three-quarters of the first round goes to close to the lower bound of the circuit which causes more energy to be lost. However, at the same time the trajectory lap in the case of the RUL objective is shorter than without the RUL criteria which makes a small trade-off between maximizing the battery RUL and optimizing the time.

According to the general control approach Fig. 2, the solution of planner optimization problem (upper layer) will be used as reference variables for the controller optimization problem (low layer). In the control optimization, the tuning aims to minimize the velocity and lateral errors while computing smooth control actions for the vehicle. The weighting matrices are founded by iterative tuning until the desired performance is achieved. The values of the parameters is used in the simulation are presented in Table 1.

Fig. 5 show the optimal results of the tracking of the trajectory path that achieved, in an online mode, by the planner without considering the RUL objective. In Fig. 5, it can seen that the controller is able perfectly to track the trajectory provided by the planner without the RUL objective. On the other side, the evaluation results of the tracking of the trajectory path using planner by considering the RUL objective are presented in Fig. 6. Moreover, it can observed that despite considering the RUL objective, the controller perfectly tracked the optimal trajectory that provided by the planner.

Fig. 7 presents the reference and the response of the longitudinal velocity profile in both scenario of the RUL objective. From this figure, it can be observed that in the scenario with RUL criteria, the response of velocity from the planner is modified based on the RUL and it is less than the velocity without the RUL criteria. In both scenarios, the results from the controller tracking part are quite good and the response of velocity have tracked the reference from the planner.

The evaluation of error during the simulation racing lap by considering SoC criteria and without it are presented in Fig. 8. In fact, The good performance of the controller tracking is shown in Fig. 8. It can be perceived that the controller is able to reduce the errors to zero in spite of the complexity of driving in a high lateral acceleration situation. The comparison of the RUL of battery between considering the RUL objective and without adding the RUL objective is presented in Fig. 9, where it can

be seen that at time (50s), the result of battery RUL with RUL objective is 11.71, while the result of battery RUL without RUL objective is zero. Therefore, It can be said, the battery RUL is increased 11.71 according to the solving the robust LMI of planner without the RUL objective.

To evaluate the effectiveness and RUL efficiency of the presented approach based on the robust LMI problem, the comparison of response of the tracking controller from the system model that includes the friction force disturbance and measurement noise with the system model without them are presented in Fig. 10. Moreover, Fig. 11 depicts the response of the longitudinal velocity profile in both scenario of the friction force disturbance and measurement noise where the level of noise considered as random value of 20% of steady-state level of velocity and friction force disturbance is shown in Fig. 12.

Furthermore, to show the differences of time scale between the upper layer and lower layer, the position of closed loop poles from both layers in a particular operating point are illustrated in Fig. 13. From this figure can be observed that the poles of both loops satisfy the stability of the system behaviors. According to using LPV model cannot be used fixed eigenvalue in closed loop but, in every iteration try to force and obtain the poles near to zero. Moreover, the poles position from the two layers are shows the dynamic behavior of lower layer is faster than upper layer.

6. Conclusions

This paper has proposed a methodology for autonomous steering a vehicle based on the robust LMI-based MPC approach. The nonlinear model of vehicle is modified by including the time and the battery model as states into the vehicle model. Then, to take into account the nonlinearities of the vehicle, the nonlinear model is transformed into an LPV model using a polytopic approach. The proposed approach is designed to solve driving control problems and at the same time to maintain and minimize the consumption of the battery energy. The proposed solution is divided into two layers with different time scale: path planner and controller. Pole placement approach is used dynamic decoupling between both layers. The optimal planning algorithm additionally minimizes the lap time while at the same time maximizes the lifetime of battery. The controller is designed using a LPV-LQR approach using LMI formulation. The model of the controller is augmented with integral action for improving the trajectory tracking obtained on-line by the planner. To evaluate the effectiveness and RUL efficiency of the presented approach, the force friction disturbance and noise is considered inside the system. The strategies are tested in simulation using the Berkeley autonomous vehicle with different scenarios including the comparison of system behaviors and battery RUL. The results show that the RUL of the battery is maximized in all scenarios. For future research, it would be interesting to consider the fault in the system and implementing the proposed approach on the real benchmark of the vehicle.

Declaration of competing interest

The authors declare that they have no known competing financial interests or personal relationships that could have appeared to influence the work reported in this paper.

Appendix

The mathematical expressions of the varying parameters in matrices A and B of the LPV model (13) are as follows

$$a_{11} = \frac{-\mu g}{v_x}, \qquad a_{13} = \frac{C_f l_f \sin(\delta)}{m v_x} + v_y,$$

$$a_{12} = \frac{C_f \sin(\delta)}{m v_x}, \qquad a_{22} = -\frac{C_r + C_f \cos(\delta)}{m v_x},$$

$$a_{23} = -\frac{C_f l_f \cos(\delta) - C_r l_r}{m v_x} - v_x, \qquad a_{32} = -\frac{C_f l_f \cos(\delta) - C_r l_r}{I v_x},$$

$$a_{33} = -\frac{C_f l_f^2 \cos(\delta) + C_r l_r^2}{I v_x}, \qquad a_{45} = v_x,$$

$$a_{52} = -\frac{\kappa}{1 - e_y \kappa}, \qquad a_{53} = \frac{\kappa \sin(e_\theta)}{1 - e_y \kappa},$$

$$a_{61} = \frac{\cos(e_\theta)}{1 - e_y \kappa}, \qquad a_{62} = -\frac{\sin(e_\theta)}{1 - e_y \kappa},$$

$$a_{71} = -\frac{1}{2} C_d \rho A_r - \mu m g, \qquad b_{11} = -\frac{1}{m} \sin(\delta) C_f,$$

$$b_{21} = \frac{1}{m} \cos(\delta) C_f, \qquad b_{31} = \frac{1}{m} \cos(\delta) C_f l_f.$$

References

[1] Ni J, Hu J. Dynamics control of autonomous vehicle at driving limits and experiment on an autonomous formula racing car. Mech Syst Signal Process 2017;90:154–74.

[2] Kang CM, Kim W, Chung CC. Observer-based backstepping control method using reduced lateral dynamics for autonomous lane-keeping system. ISA Trans 2018;83:214–26.

[3] Brookhuis KA, De Waard D, Janssen WH. Behavioural impacts of advanced driver assistance systems–an overview. Eur J Transp Infrastruct Res 2019;1(3).

[4] Hu X, Chen L, Tang B, Cao D, He H. Dynamic path planning for autonomous driving on various roads with avoidance of static and moving obstacles. Mech Syst Signal Process 2018;100:482–500.

[5] Gandolfo DC, Salinas LR, Serrano ME, Toibero JM. Energy evaluation of low-level control in UAVs powered by lithium polymer battery. ISA Trans 2017;71:563–72.

[6] Dolgov D, Thrun S, Montemerlo M, Diebel J. Path planning for autonomous vehicles in unknown semi-structured environments. Int J Robot Res 2010;29(5):485–501.

[7] Xu W, Pan J, Wei J, Dolan JM. Motion planning under uncertainty for on-road autonomous driving. In: 2014 IEEE international conference on robotics and automation. IEEE; 2014, p. 2507–12.

[8] Shum A, Morris K, Khajepour A. Direction-dependent optimal path planning for autonomous vehicles. Robot Auton Syst 2015;70:202–14.

[9] Rasekhipour Y, Khajepour A, Chen S-K, Litkouhi B. A potential field-based model predictive path-planning controller for autonomous road vehicles. IEEE Trans Intell Transp Syst 2016;18(5):1255–67.

[10] El Hajjaji A, Bentalba S. Fuzzy path tracking control for automatic steering of vehicles. Robot Auton Syst 2003;43(4):203–13.

[11] Fan Z, Chen H. Study on path following control method for automatic parking system based on LQR. SAE Int J Passenger Cars-Electronic Electr Syst 2016;10(2016-01-1881):41–9.

[12] Raffo GV, Gomes GK, Normey-Rico JE, Kelber CR, Becker LB. A predictive controller for autonomous vehicle path tracking. IEEE Trans Intell Transp Syst 2009;10(1):92–102.

[13] Alcala E, Puig V, Quevedo J, Escobet T. Gain-scheduling LPV control for autonomous vehicles including friction force estimation and compensation mechanism. IET Control Theory Appl 2018;12(12):1683–93.

[14] Németh B, Gáspár P, Bokor J. LPV-Based integrated vehicle control design considering the nonlinear characteristics of the tire. In: 2016 American control conference (ACC). IEEE; 2016, p. 6893–8.

[15] Pour FK, Puig V, Ocampo-Martínez C. Economic predictive control of a pasteurization plant using a linear parameter varying model. In: Computer aided chemical engineering, vol. 40. Elsevier; 2017, p. 1573–8.

[16] Ji J, Khajepour A, Melek WW, Huang Y. Path planning and tracking for vehicle collision avoidance based on model predictive control with multiconstraints. IEEE Trans Veh Technol 2016;66(2):952–64.

[17] Erlien SM. Shared vehicle control using safe driving envelopes for obstacle avoidance and stability. (Ph.D. thesis), Stanford University; 2015.

[18] Jiang X, Motai Y, Zhu X. Predictive fuzzy control for a mobile robot with nonholonomic constraints. In: ICAR'05. Proceedings., 12th international conference on advanced robotics, 2005. IEEE; 2005, p. 58–63.

[19] Gu D, Hu H. Neural predictive control for a car-like mobile robot. Robot Auton Syst 2002;39(2):73–86.

[20] Rosolia U, Carvalho A, Borrelli F. Autonomous racing using learning model predictive control. In: 2017 American control conference (ACC). IEEE; 2017, p. 5115–20.

[21] Bujarbaruah M, Zhang X, Tseng HE, Borrelli F. Adaptive MPC for autonomous lane keeping. 2018, arXiv preprint arXiv:1806.04335.

[22] Verschueren R, Zanon M, Quirynen R, Diehl M. Time-optimal race car driving using an online exact hessian based nonlinear MPC algorithm. In: 2016 European control conference (ECC). IEEE; 2016, p. 141–7.

[23] Brunner M, Rosolia U, Gonzales J, Borrelli F. Repetitive learning model predictive control: An autonomous racing example. In: 2017 IEEE 56th annual conference on decision and control (CDC). IEEE; 2017, p. 2545–50.

[24] Tang L, Hettler E, Zhang B, DeCastro J. A testbed for real-time autonomous vehicle PHM and contingency management applications. In: Annual conference of the prognostics and health management society. 2011, p. 1–11.

[25] Niu G, Jiang J, Youn BD, Pecht M. Autonomous health management for PMSM rail vehicles through demagnetization monitoring and prognosis control. ISA Trans 2018;72:245–55.

[26] Karimi Pour F, Puig V, Cembrano G. Health-aware LPV-mpc based on a reliability-based remaining useful life assessment. IFAC-PapersOnLine 2018;51(24):1285–91.

[27] Sankararaman S, Daigle M, Saxena A, Goebel K. Analytical algorithms to quantify the uncertainty in remaining useful life prediction. In: 2013 IEEE aerospace conference. IEEE; 2013, p. 1–11.

[28] Watrin N, Blunier B, Miraoui A. Review of adaptive systems for lithium batteries state-of-charge and state-of-health estimation. In: 2012 IEEE transportation electrification conference and expo (ITEC). IEEE; 2012, p. 1–6.

[29] Zhong Q, Zhong F, Cheng J, Li H, Zhong S. State of charge estimation of lithium-ion batteries using fractional order sliding mode observer. ISA Trans 2017;66:448–59.

[30] Nuhic A, Terzimehic T, Soczka-Guth T, Buchholz M, Dietmayer K. Health diagnosis and remaining useful life prognostics of lithium-ion batteries using data-driven methods. J Power Sources 2013;239:680–8.

[31] Saha B, Goebel K. Modeling Li-ion battery capacity depletion in a particle filtering framework. In: Proceedings of the annual conference of the prognostics and health management society; 2009. p. 2909–924.

[32] Li F, Xu J. A new prognostics method for state of health estimation of lithium-ion batteries based on a mixture of Gaussian process models and particle filter. Microelectron Reliab 2015;55(7):1035–45.

[33] Zhang J, Lee J. A review on prognostics and health monitoring of li-ion battery. J Power Sources 2011;196(15):6007–14.

[34] Plett GL. Sigma-point kalman filtering for battery management systems of LiPB-based HEV battery packs: Part 1: Introduction and state estimation. J Power Sources 2006;161(2):1356–68.

[35] Schacht-Rodriguez R, Ortiz-Torres G, Garcia-Beltran C, Astorga-Zaragoza C, Ponsart J-C, Theilliol D. SoC Estimation using an extended Kalman filter for UAV applications. In: 2017 international conference on unmanned aircraft systems (ICUAS). IEEE; 2017, p. 179–87.

[36] Karimi Pour F, Puig V, Cembrano G. Health-aware LPV-mpc based on system reliability assessment for drinking water networks. In: 2018 IEEE conference on control technology and applications (CCTA). IEEE; 2018, p. 187–92.

[37] Langeron Y, Grall A, Barros A. Joint maintenance and controller reconfiguration policy for a gradually deteriorating control system. Proc. Inst. Mech. Eng. O 2017;231(4):339–49.

[38] Rodriguez DJ, Martinez JJ, Berenguer C. An architecture for controlling the remaining useful lifetime of a friction drive system. IFAC-PapersOnLine 2018;51(24):861–6.

[39] Boyd S, El Ghaoui L, Feron E, Balakrishnan V. Linear matrix inequalities in system and control theory, vol. 15. Siam; 1994.

[40] Araújo HX, Conceição AG, Oliveira GH, Pitanga J. Model predictive control based on LMIs applied to an omni-directional mobile robot. IFAC Proc Vol 2011;44(1):8171–6.

[41] Pacejka H. Tire and vehicle dynamics. Elsevier; 2005.

[42] Kwiatkowski A, Boll M, Werner H. Automated generation and assessment of affine LPV models. In: Proceedings of the 45th IEEE conference on decision and control 2006. p. 6690–95.

[43] Karimi Pour F, Puig V, Ocampo-Martinez C. Multi-layer health-aware economic predictive control of a pasteurization pilot plant. Int J Appl Math Comput Sci 2018;28(1):97–110.

[44] Bianco C, Piazzi A, Romano M. Velocity planning for autonomous vehicles. In: IEEE intelligent vehicles symposium, 2004. IEEE; 2004, p. 413–8.

[45] Kothare MV, Balakrishnan V, Morari M. Robust constrained model predictive control using linear matrix inequalities. Automatica 1996;32(10):1361–79.

[46] Duan G-R, Yu H-H. LMIs in control systems: analysis, design and applications. CRC press; 2013.

[47] Chilali M, Gahinet P. H/sub/spl infin//design with pole placement constraints: an lmi approach. IEEE Trans Autom Control 1996;41(3):358–67.